Soil Corrosion of the AISI1020 Steel Buried Near Electrical Power Transmission Line Towers

Anderson de Oliveira Fraga[a], Marcos Antonio Klunk[a], Adriano Agnoletto de Oliveira[b],

Gilnei Gonçalves Furtado[b], Gerhard Knörnschild[a], Luís Frederico Pinheiro Dick[a]*

[a]Laboratório de Processos Eletroquímicos & Corrosão – ELETROCORR, Departamento de Metalurgia, Universidade Federal do Rio Grande do Sul – UFRGS. Av. Bento Gonçalves, 9500, Bloco 4, Prédio 75, CEP 91501-970, Porto Alegre, RS, Brasil
[b]Companhia de Energia Elétrica Estadual – CEEE, Av. Joaquim Porto Villanova, 201, Prédio F, sala 205, Porto Alegre, RS, Brasil

Soil corrosion of carbon steel samples buried up to hundred days close to a high voltage power transmission line tower was examined by weight loss vs. time. A higher weight loss was observed if the samples were electrically connected to the tower than if they were not. This was attributed to the influence of alternating current (AC) signals induced in the soil by the transmission line. This field study showed for the first time the influence of the AC power line on the buried structure of the tower, while other studies so far were focused only on AC corrosion of cathodically protected coated pipelines, running parallel to the transmission line. An improved method was used to measure weight loss by descaling in Clark solution. The new method substitutes discontinuous measurements, proposed in the ASTM-G1-90 standard, by *in situ* measurements of the weight loss during descaling, using a computer controlled microbalance.

Keywords: *soil corrosion, weight loss, AC corrosion, chemical descaling*

1. Introduction

Alternating current (AC) induced corrosion is subject of scientific research since it has been observed that the soil corrosion of buried metallic structures under certain circumstances is accelerated by the influence of AC signals[1-4]. It had been formerly assumed that only the direct current (DC) component of an alternating signal could cause corrosion damage. However, a growing number of corrosion cases was observed at buried pipelines, which were installed in short distance and parallel to high voltage AC transmission lines or to electrified railways[1-3]. Damage could obviously occur even when the pipeline was provided with a cathodic protection system. Some researchers attributed the AC influence on corrosion to a rectification current, which can be expected as the result of an asymmetric Tafel behavior[5-6].

According to Goidanich et al.[7], AC signals have influence on the kinetic parameters of anodic and cathodic reactions and lead to modification of corrosion potential (E_{corr}) and corrosion current density (i_{corr}) values. In most cases, a shift of E_{corr} to more negative values and a higher i_{corr} are reported[7-8]. The results, however, depend on the electrode material, the electrolyte and the height of the AC signal. Even a decrease of i_{corr} under AC influence was found in one case[7]. Laboratory tests in simulated soil medium showed that the current efficiency with respect to weight loss is much lower in the case of AC than in the case

of DC.[7] According to the literature the current efficiency is below 5% and depends on the amplitude of the AC signal[9]. Nevertheless, some authors attributed corrosion rates as high as 1mm/y to AC-corrosion during the first year of exposure[5], probably diminishing during further exposure. An important point of discussion is the question in which way weight loss is related to AC and if other parameters must be taken into account in order to define safe operational conditions for buried constructions[10]. In this context, the interaction of AC with imposed cathodic protection currents was discussed[10]. At cathodic current densities oxygen reduction leads to alkalinization of the metal surface. High cathodic protection currents combined with high AC component can cause the formation of soluble iron hydrates. Dissolution of one monolayer during one AC cycle would mean a corrosion rate of 70mm/y[11]. Redox reactions between Fe^{2+} and Fe^{3+} in the iron oxide films take place during the positive and negative half wave and lead to the formation and reductive dissolution of protective passive films and non-protective rust films[11]. Goidanich et al.[7] confirmed that AC leads to the growth of thick but non-adherent films of corrosion products on the metal surface and that, in this way, AC enhances localized corrosion. The authors found that nature, thickness and adhesion of the film changes with AC density, type of metal and solution composition. Brenna[12] suggested that AC causes the electro-mechanical breakdown of the passive film formed on the metal surface under cathodic protection conditions and corrosion occurs after passive film

*e-mail: lfdick@ufrgs.br

breakdown if the pH at the metal-to-electrolyte interface is close to 14. Based on the possible interaction of AC with DC for cathodic protection authors suggested a new potential values for cathodic protection, which would depend on the AC signal to which the structure is exposed[13]. Others believe that cathodic protection is difficult in these cases and that mitigation of the AC influence would be a better approach[14-15].

AC induced corrosion of buried coated steel pipelines under cathodic protection to prevent corrosion at coating failures has attracted attention due to its economic importance, while other buried metal structures, which also might be subject to AC induced corrosion damage, have been much less studied[16]. Among them are the metallic structures of the high voltage transmission lines itself. The buried base of the power line towers consists of galvanized carbon steel and soil corrosion of this part might be accelerated by signals induced from the power line. Electric fields due to uncompensated AC phases at the ground between two towers are estimated to values around 4 kV/m beneath lines with voltages from 110kV to 380kV.[17] Moreover, influence can originate from stray currents and from atmospheric discharges. Wojcicki[18] suggested that stray currents originate in the lightning rod cables of the power line towers and flow through the ground to close the loop to the neighboring tower. Potential measurements of the tower *versus* a buried Cu/CuSO$_4$ reference electrode, made between the lightning rod and the neighboring tower showed in many cases that the potential becomes more negative towards the tower. This shows that an anodic current flows off the tower surface, indicating its corrosion[18]. To our best knowledge, studies dedicated to determine the rate of this corrosion and a possible influence on it of AC signals from the transmission line do not exist so far.

Therefore, in the present work, soil corrosion of carbon steel was examined by field studies with samples buried near a high voltage power transmission line tower. To evaluate the influence of induced AC signals, the electrical potential of one part of the samples was equalized to the potential of the tower by electrically connecting sample and tower. The weight loss of samples electrically connected to the tower was measured *vs.* time and compared with samples without electric contact.

2. Experimental Procedures

Studies of soil corrosion were performed with AISI 1020 (UNS G10200)[19] carbon steel coupons with the dimensions of 70 × 20 × 2 mm and provided with a hole of 2mm diameter at the upper part. These samples were sequentially ground on all sides with emery papers of granulometry up to 4000 mesh. The studies were performed near a power transmission tower located in *Porto Alegre*, Brazil, at the area of the *Rio Grande do Sul Electric Energy State Company* (CEEE). The transmission tower was chosen for tests because of its protected location with access restricted to company employees. The soil to which the steel samples were exposed had a chloride concentration of 7.0mg/kg, a sulfate concentration of 3.0mg/kg and a pH value of 6.4 and a mean resistivity around 10kΩ.cm. Half of the samples was electrically connected to the transmission tower by an isolated copper wire, while the other half was not connected to the tower. Connected and unconnected samples were buried close to each other (≈ 1m) at 25 cm below the surface and tests were performed in parallel. The samples remained exposed to the soil for periods ranging from nine to one hundred days during the winter (June-September). The mean relative humidity, which is rather constant in Porto Alegre varied during the exposure time between 78 and 82%, the mean daily temperature between 14.7 to 16.8 °C, and the pluviometric precipitation between 110 and 180 mm/month. After withdrawal of the samples, loosely adherent particles were removed and weight loss was determined by immersion of samples in Clark solution, as described in the ASTM G1-90 standard[20]. Weight loss by dissolution of the corrosion products was monitored *in situ*, while the samples were immersed in Clark solution. For this purpose, samples were hanged on a frame connected to an analytical balance with a resolution of 100μg provided with a RS232 interface for data acquisition and calculation of weight loss during dissolution of oxides (Figure 1). DC and AC components of the samples´ potentials were measured against a saturated CuSO$_4$/Cu electrode in contact with the soil by a flat sponge soaked with saturated CuSO$_4$ solution, using a voltmeter and a *Rigol OS1025* oscilloscope. Potentials were measured for connected and unconnected samples positioned close to the tower, as well as for samples distant from the tower.
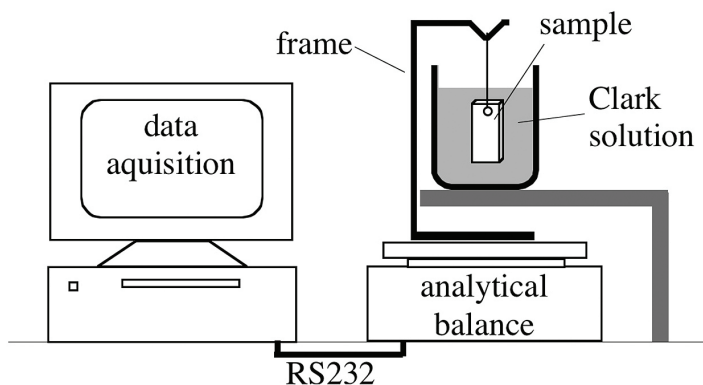

Figure 1. Experimental scheme for *in situ* weight loss measurements during oxide dissolution of corroded samples in Clark solution.

The Raman spectra of the corrosion products were examined with a *Dilor–Jobin Yvon* spectrophotometer attached to an *Olympus BX60M* optical microscope. The laser power on the samples was 9mW, using the 632.82nm line of a He–Ne laser. All spectra were recorded using a pinhole with a diameter of 1000μm, resulting from three accumulations of 5s without filters.

3. Results and Discussion

Figure 2 shows a weight loss *versus* time curve obtained during immersion of corroded samples in Clark solution. Purpose of this solution, defined by ASTM G1-90 standard[20], is the dissolution of solid corrosion products formed during exposure to the soil. Clark solution according to ASTM G1-90 consists of HCl, Sb_2O_3 and $SnCl_2$. Singh et al.[21] describe the function of its ingredients as follows: Sb_2O_3 acts as inhibitor for acid corrosion of steel and has an efficiency of 98%. Oxides are dissolved by HCl, according to:

$$Fe_2O_3 + 6HCl_{aq} \rightarrow 2\ FeCl_{3\ aq} + 3H_2O \qquad (1)$$
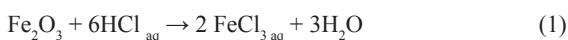
$SnCl_2$ is thought to accelerate oxide dissolution by reduction of Fe^{3+}, thus shifting the equilibrium of Equation (1) to the right side, according to Equation (2):

$$2Fe^{3+}_{aq} + Sn^{2+}_{aq} \rightarrow 2Fe^{2+}_{aq} + Sn^{4+}_{aq} \qquad (2)$$
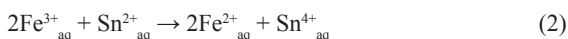
The initially faster weight loss in Figure 2 can be attributed to the chemical dissolution of corrosion products. When uncovered, bare metal surface is exposed, the dissolution rate slows down due to inhibition of the acid corrosion and also oscillates. Evolution and detachment of adhered H_2 bubbles were observed at this phase and explains the weight oscillation during an electrochemical process of metal dissolution. A self-developed computer program fitted in real-time the acquired weight data during dissolution

in the Clark solution with two straight lines, one for the processes of chemical dissolution of corrosion products and another of the acid corrosion of the steel substrate, respectively. The oxide-weight loss was determined from the intersection of these two lines, as shown in Figure 2 and corrected for the buoyancy due to solution displacement by Equation (3a) and converted into metal loss by Equation (3b) as explained below.

The weight loss measured during dissolution in the Clark solution must be corrected by discounting the buoyancy due to solution displacement. For the case that only oxide is dissolved it can be shown that the actual weight loss ΔP_{Ox} is given by:

$$\Delta P_{Ox} = \Delta P_{meas} \cdot \rho_{Ox} / (\rho_{Ox} - \rho_{Sol}) = k \cdot \Delta P_{meas} \qquad (3a)$$

where ΔP_{meas} is the measured weight loss during dissolution, ρ_{Sol}, the specific weight of the Clark solution ($1.26\ g \cdot cm^3$)[20], ρ_{Ox}, the specific weight of the oxide and k, a coefficient as defined in Equation (3a). Assuming that only lepidocrocite (γ-FeOOH) is formed as corrosion product with a specific weight $\rho_{lepidocrocite} = 4.09 \pm 0.04\ g \cdot cm^{-3}$[22] the constant k in Equation (3) would be 1.45, while for the formation of goethite (α-FeOOH, $\rho_{goethite} = 4.28 \pm 0.05\ g \cdot cm^{-3}$)[23] k would change to 1.42. The α/γ relation reported for the corrosion products formed by the atmospheric corrosion of carbon steel ranges from 0.74 to 0.97, besides the formation of amorphous FeOOH[24]. Assuming a α/γ ratio ≈ 1 and that the density of amorphous FeOOH is close to that of α and γ, a mean value of $k = 1.435$ can be assumed with an error lower than 2%.

From the weight gain of Fe-oxide formation, as determined using Equation (3a) for the oxide dissolution in Clark solution, the weight loss of Fe due to soil corrosion, ΔP_{Fe}, can be calculated as follows:
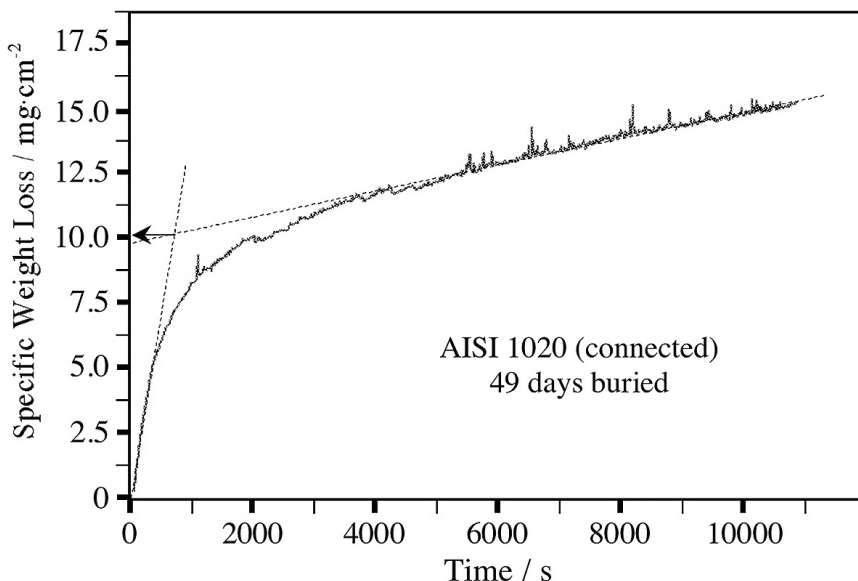

Figure 2. *In situ* measurement of specific weight loss during exposure of corroded sample to Clark solution.

$$\Delta P_{Fe} = (M_{Fe}/M_{FeOOH}) \cdot \Delta P_{meas} \cdot \rho_{Ox}/(\rho_{Ox} - \rho_{Sol}) = 0{,}902 \cdot \Delta P_{meas} \quad \text{(3b)}$$

where M_{Fe} and M_{FeOOH} are the molar masses of Fe and FeOOH. If only Fe is being dissolved by the Clark solution, as expected for the second part of the dissolution curve of Figure 2, then k in Equation (3a) will assume a value of 0.83.

Figure 3 shows the weight loss of samples exposed during a period up to 100 days in the soil. Each point of the diagram represents the average of three measurements. The weight gain of samples connected to the transmission tower is higher than the one shown by unconnected ones. Weight loss by oxide formation of both, connected and unconnected samples follows a time law of exponent lower than one. This becomes more evident in the comparison of corrosion rates in Figure 4, calculated from the slopes $(\Delta M/A)/Dt$ at each time interval in Figure 3. The diagram shows that the differences between connected and unconnected samples are higher for short exposure times. Nevertheless, the corrosion rate of the samples connected to the tower remains higher during the whole period of test, revealing a possible influence of AC signals induced by the transmission tower. The corrosion attack at the buried samples is not uniform. When only the attacked area determined by optical inspection is considered for the weight loss per area, the

differences between connected and unconnected samples become higher for short exposure periods, as seen in Figure 5. This means that initially a smaller area is attacked at the connected samples. During the entire exposure period of 100 days the corrosion attack spreads laterally over nearly the whole surface (Figure 6, right side). The mean corrosion rate related to the attacked area decreases with the exposure time (Figure 6, left side), thus diminishing the differences between weight losses per geometric (Figure 3) and per attacked area (Figure 5). This behavior is in agreement with the results of other authors, which reported a tendency to more localized corrosion attack in cases of AC corrosion[24].

Measurements of the alternating part of the electrode potential of buried samples showed a strong influence from the 60 Hz signal of the transmission line. The highest amplitude with this frequency, 3.64V, was measured with samples connected to the tower (Table 1). The amplitude diminished about twenty times when the sample was located close to the tower (about 1m), but electrically isolated from it. At a distance of 30 meters from the tower the 60 Hz signal disappeared and only weak signals in the hundreds of kHz range were observed, which can be attributed to induced radio signals. Measured DC corrosion potentials of the steel samples buried 30m from the tower and of a sample
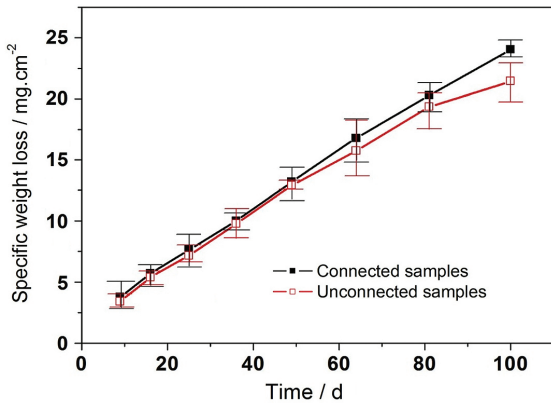

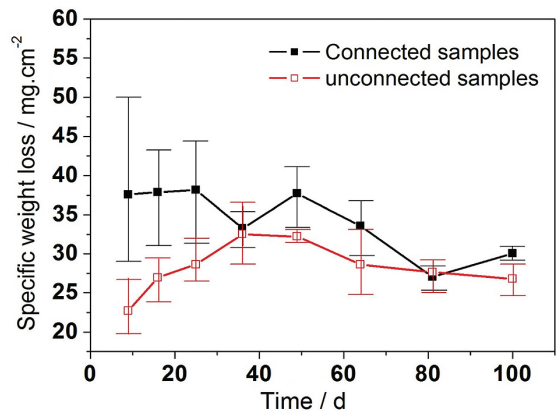**Figure 3.** Specific weight loss per geometric area *versus* exposure time.

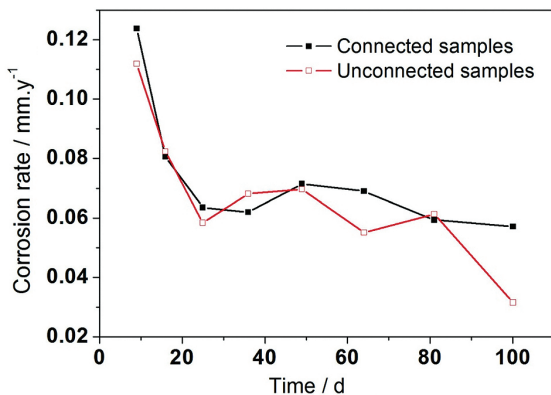**Figure 5.** Specific weight loss per attacked area *versus* exposure time.

Figure 4. Corrosion rate during exposure time of buried samples related to the geometric surface area.
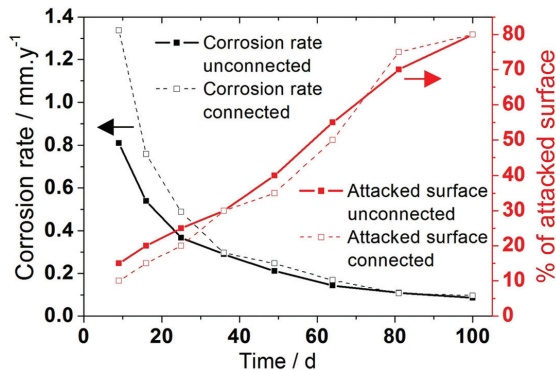

Figure 6. Mean corrosion rate during exposure time per attacked surface and percentage of attacked surface *versus* total exposure time.

buried in a similar soil at approximately 1km far from transmission lines, were –0.280V (SHE) and –0.200V(SHE), respectively. In comparison with these potentials, which can be considered as reference values for samples not influenced by AC-corrosion, the corrosion potentials were higher when the sample was buried close to the tower, and still higher when it was electrically connected to the tower. It is evident in the case of the connected samples that under the influence of the AC-signal the galvanized steel base of the tower has no protective effect on the sample. According to the rectification model[5,6] the AC influence on the corrosion potential depends on whether the ratio of cathodic to anodic Tafel slopes ba/bc is >1 or <1. Measurements from Goidanich et al.[7] with carbon steel in soil-simulating electrolyte showed ba/bc < 1, which is plausible for a partially transport controlled cathodic reaction and an anodic attack with localized character. For the case ba/bc <1, the theory predicts a shift of the corrosion potential to more negative values under the influence of AC. However, as in the present field study

of soil corrosion, Goidanich et al.[7] found under laboratory conditions for samples immersed in simulated soil solution a shift of the corrosion potential to more positive values. In accordance with our results, weight loss tests from Goidanich et al.[25] confirmed that the higher corrosion potential under AC influence led to a higher corrosion rate. The authors mentioned that other results of their work, like independence of current efficiency from experimental conditions are also in conflict with a simple rectification theory of AC corrosion[7,25].

While Goidanich et al.[7,25] made tests in well-defined soil simulating electrolytes, soil corrosion in the present study is determined by the combination of a variety of soil parameters and additionally by the climate conditions the soil is exposed to during the corrosion tests. In field tests, local inhomogeneities of the soil and varying climate conditions can lead to the scattering of the results. In the present study, the error caused by soil inhomogeneities was kept small by burying connected and unconnected samples

Table 1. In-situ AC/DC measurements in the soil.

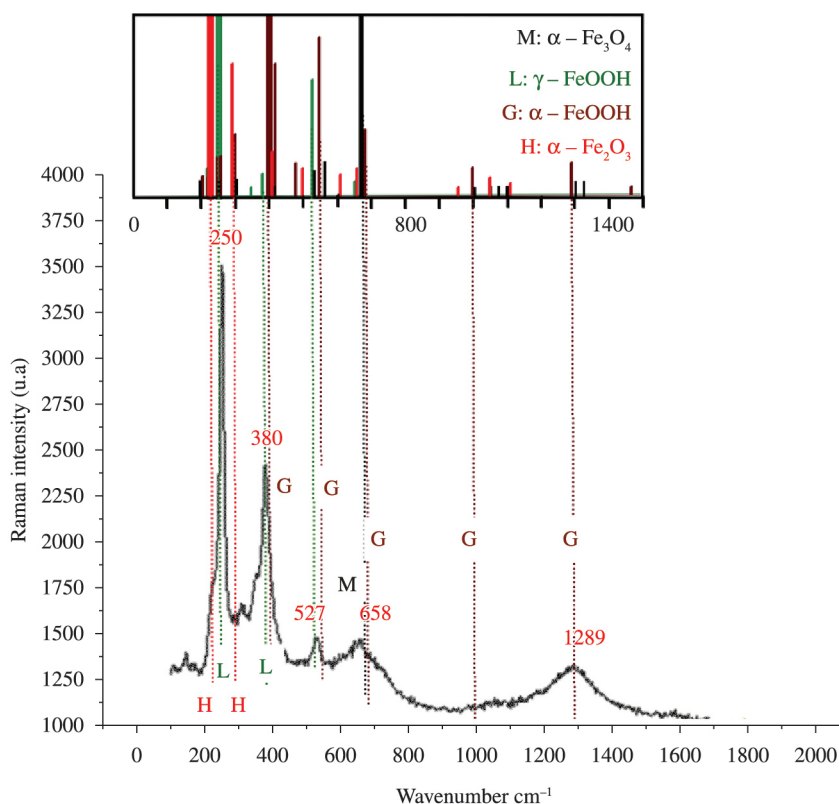|	Sample connected to the tower	Sample beneath the tower, unconnected	Sample at 30m from the tower	Sample at very long distance in similar soil
Frequency	60.2Hz	62.5Hz	~10²kHz range	---
AC-Amplitude	3.64V	0.20V (spikes 2.2V)	< 10mV	---
DC-Corrosion Potential	–0.050V(SHE)	–0.165V(SHE)	-0.280V(SHE)	-0.200V(SHE)

Figure 7. Raman spectrum of the corrosion products for AISI 1020 exposed during 64 days connected to the power line tower. Insert: Schematic normalized Raman spectra of lepidocrocite (L), goethite (G), magnetite (M) and hematite (H).

close to each other. By performing the tests with the two types of samples simultaneously the weather conditions were the same for both types. The measurement of weight loss was made with a computer controlled *in situ* method. It can be expected that this method gives better results than descaling analysis based on optical inspection with naked eye. Singh et al.[21] reported that a weak point of weight loss determinations described by-ASTM G1-90[20] is that different types of steel show different rates of acid corrosion in the Sb_2O_3 inhibited solution. Since in our work all measurements were performed with the same steel, errors are expected to have the same effect on connected and on unconnected samples. The same statement can be made with respect to the influence of the weather conditions. It can therefore be assumed that the measured differences between connected and unconnected samples are due to the influence of an induced AC signal.

Although pH, chloride and sulfate concentration and the resulting resistivity of the soil at the test location are considered between mildly and very mildly corrosive, according to ASTM G187-12[26], the mean corrosion rate during 100 days is nearly one order of magnitude above the value considered acceptable for buried pipelines under cathodic protection (0,01mm/year). The measured values are in reasonable agreement with weight loss measurements from Barbalat et al.[27], who found a corrosion rate around 0,1mm/year during 75 days in a soil with similar characteristics.

Figure 7 shows the Raman shift spectra acquired on the AISI 1020 after an exposure time of 64 days connected to the power line tower. Normalized schematic Raman spectra of possible corrosion products were extracted from the literature[28] and plotted schematically on the insert of Figure 7. Similarly to what is observed for other cases of corrosion of carbon steel, such as corrosion in humid atmospheres[24], in aerated solutions[29], as well as soil corrosion of unpolarized buried steel[30], the main corrosion product observed in the present work was lepidocrocite

(γ-FeOOH) followed by goethite (a-FeOOH) and in a lower intensity also magnetite (α-Fe_3O_4). No significant differences could be observed between Raman spectra of connected and unconnected samples under the influence of induced AC signal.

4. Conclusions

It is today generally accepted in the scientific community that AC signals from high voltage power lines can influence the corrosion of nearby installed protected metallic structures like pipelines. In these cases locally high current densities might pass through small defects of the protective coatings. While it seems to be consolidated that the rate of AC corrosion increases with the increase of the amplitude of AC density, thus predicting risks for damaged coatings, the existence of a safe lower limit of the amplitude is still in question. Equivalent studies of the AC influence on the metallic structure of the transmission towers itself had not been reported so far in the literature. Our field studies have qualitatively shown that the AC signal can also influence the corrosion of the buried metallic structure of the transmission tower, although the AC is not confined to coating defects and might have, therefore, a much lower amplitude.

The tests with AISI1020 steel samples simulate a situation when the buried galvanized steel structure of the tower has already lost its zinc protection and accelerated corrosion of the ferrous base material takes place. Corrosion rates, measured by weight loss, were above the acceptable lower limit for buried metal structures. To quantify the real risks that emanate from the AC influence, the local signal has to be monitored and controlled lab tests with similar conditions have to be performed.

References

1. Heim G, Peez G. Wechselstrombeeinflussung einer kathodisch geschützten Erdgashochdruckleitung. *3R International.* 1988; 27:345-351.

2. Helm G, Heim Th, Heinzen H, Schwenk W. Investigation of corrosion of cathodically protected steel subjected to alternating currents. *3R International.* 1993; 32(5):246-250.

3. Bindschedler D, Stalder F. Wechselstrominduzierte Korrosionsangriffe auf eine Erdgasleitung. *Gas, Wasser, Abwasser: GWA*. 1991; 71:307-313.

4. Kirkpatrick EL. Basic concepts of induced alternating current voltages on pipelines. *Materials Performance*. 1995; 34:14-18.

5. Bertocci U. AC induced corrosion: the effect of an alternating voltage on electrodes under charge-transfer control. *Corrosion*. 1979; 35(5):211-215. http://dx.doi.org/10.5006/0010-9312-35.5.211.

6. Lalvani SB and Lin X. A revised model for predicting corrosion of materials induced by alternating voltages. *Corrosion Science*. 1996; 38(10):1709-1719. http://dx.doi.org/10.1016/S0010-938X(96)00065-0.

7. Goidanich S, Lazzari L and Ormellese MAC. Corrosion. Part 1: effects on overpotentials of anodic and cathodic processes. *Corrosion Science*. 2010; 52(2):491-497. http://dx.doi.org/10.1016/j.corsci.2009.10.005.

8. Jones DA. Effect of alternating current on corrosion of low alloy and carbon steels. *Corrosion*. 1978; 34(12):428-433. http://dx.doi.org/10.5006/0010-9312-34.12.428.

9. Pourbaix A, Carpentiers P and Gregor R. Detection of AC corrosion. In: Eurocorr 2001; 2001; Riva del Garda, Italy. 2001. Paper 228.

10. Büchler M, Schöneich H-G and Stalder F. Discussion of criteria to assess the alternating current corrosion risk of cathodically protected pipelines. In: Proceedings of the 15th Joint Technical Meeting on Pipeline Research; 2005; Orlando, USA. Pipeline Research Council International; 2005. Paper 26.

11. Büchler M, Voûte C-H and Joos D. Effect of variation of cathodic protection level over time on the a.c. corrosion process. In: CEOCOR International Congress; 2012; Luzerne, Switzerland. 2012. Paper 19.

12. Brenna A, Lazzari L and Ormellese M. AC interference corrosion of carbon steel in cathodic protection conditions:

a two-steps-mechanism. In: Eurocorr 2013; 2013; Estoril, Portugal. 2013. Paper O-1672.

13. Fu AQ and Cheng YF. Effect of alternating current on corrosion and effectiveness of cathodic protection of pipelines. *Canadian Metallurgical Quarterly.* 2012; 51(1):81-90. http://dx.doi.org/10.1179/1879139511Y.0000000021.

14. Pourbaix A, Tribollet B and Nogueira R. Interpretation of instantaneous true potentials in ac induced corrosion. In: Eurocorr 2013; 2013; Estoril, Portugal. 2013. Paper O-1293.

15. Sibila J. Mitigation of alternating current interference on buried steel pipeline. In: Eurocorr 2013; 2013; Estoril, Portugal. 2013. Paper O-1488.

16. Collet E, Delores B, Gabillard M and Ragault I. C Corrosion due to AC influence of very high voltage power lines on polyethylene-coated steel pipelines: evaluation of risks: preventive measures. *Anti-Corrosion Methods and Materials.* 2001; 48(4):221-226. http://dx.doi.org/10.1108/EUM0000000005629.

17. Wigdor M. *Electric fields under power lines: supplement to an examination of electric field under EHV overhead power transmission lines*. Silver Spring: Office of Radiation Programm, US Environmental Protection Agency; 1980.

18. Wojcicki FR, Negrisoli MEM, Franco CV. Stray current induced corrosion in lightning rod cables of 525 kV power lines towers: a case study. *Revista de Metalurgia.* 2003; 39:124-128.

19. American Iron and Steel Institute – AISI. *AISI 1020 (UNS G10200) specification*. In: Society of Automotive Engineers, editor. *SAE Handbook*. Warrendale; 1986.

20. American Society for Testing and Materials – ASTM. *ASTM G1-90: standard practice for preparing, cleaning and evaluation corrosion test specimens*. Philadelphia; 1992.

21. Singh DDN and Kumar A. A Fresh look at ASTM G1-90 Solution Recommended for Cleaning of Corrosion Products Formed on Iron and Steels. *Corrosion.* 2003; 59(11):1029-1036. http://dx.doi.org/10.5006/1.3277521.

22. Mindat. *Lepidocrocite*. Available from: <http://www.mindat.org/min-2379.html>. Access in: 31/05/ 2014.

23. Mindat. *Goethite*. Available from: <http://www.mindat.org/min-1719.html>. Access in: 31/05/ 2014.

24. Katsuhiko A. Characterization of rust layers on a plain-carbon steel and weathering steels exposed to industrial and coastal atmosphere for years. In: Waseda Y and Suzuki S, editors. *Advances in materials research: characterization of corrosion products on steel surfaces*. Berlin: Springer; 2006.

25. Goidanich S, Lazzari L and Ormellese MAC. Corrosion. Part 2: parameters influencing corrosion rate. *Corrosion Science.* 2010; 52(3):916-922. http://dx.doi.org/10.1016/j.corsci.2009.11.012.

26. American Society for Testing and Materials – ASTM. *ASTM G187-12a: standard test method for measurement of soil resistivity using the two-electrode soil box method*. West Conshohocken; 2012.

27. Barbalat M, Lanarde L, Caron D, Meyer M, Vittonato J, Castillon F, et al. Electrochemical study of the corrosion rate of carbon steel in soil: Evolution with time and determination of residual corrosion rates under cathodic protection. *Corrosion Science*. 2012; 55:246-253. http://dx.doi.org/10.1016/j.corsci.2011.10.031.

28. Downs RT. The RRUFF Project: an integrated study of the chemistry, crystallography, Raman and infrared spectroscopy of minerals. In: Program and Abstracts of the 19th General Meeting of the International Mineralogical Association; 2006; Kobe, Japan. 2006. O03-13.

29. Misawa T, Hashimoto K and Shimodaira S. The mechanism of formation of iron oxide and oxyhydroxides in aqueous solutions at room temperature. *Corrosion Science*. 1974; 14(2):131-149. http://dx.doi.org/10.1016/S0010-938X(74)80051-X.

30. Córdoba vc, Mejía MA, Echeverría F, Morales M and Calderón JA. Corrosion mitigation of buried structures by soils modification. *Ingeniare: Revista Chilena de Ingeniería*. 2011; 19(3):486-497.